Proceedings of the
Annual Stability Conference
Structural Stability Research Council
St. Louis, Missouri, April 2-5, 2019

Strengthening beam sections of industrial buildings against lateral torsional buckling

Sepehr Movaghati[1]

Abstract
Crane bridge girders and runway beams in industrial buildings are susceptible to lateral torsional buckling. When there is an interest to increase the rated capacity of a crane, these beams should be strengthened for the new load values. Welding additional steel members to a slender beam section is a method to increase the load-bearing capacity of the original beam. However, current beam design guidelines and steel design codes do not extensively address the lateral torsional buckling resistance of complex built-up and asymmetric steel sections. The objective of this analytical study is to investigate the effect of welding additional angle sections to the compression flange tips in order to increase the load-bearing capacity of rolled I-shape beams. To compare the original sections with the strengthened sections, finite element models are developed using shell elements. For the evaluated I-shaped sections, the lateral torsional buckling resistance of the beams is at least three times greater when the additional angles have been installed.

1. Introduction

In industrial buildings, the compression flange in monorail crane bridge girders and runway beams are not laterally braced (Fig 1.). These beam members with a long torsional unbraced length, are under biaxial flexure load caused by the vertical lifting load and crane dead load, as well as the lateral and longitudinal impact loads. Therefore, they may fail under overall lateral torsional buckling (LTB) before the inelastic bending behavior.

In many industrial buildings, there is an interest to increase the lifting capacity of cranes. Replacing the crane bridge girder with a stronger new girder, couple the bride girder with an additional girder or adding a new column at the midspan of the runway beams are not the most economical solutions for this purpose. The runway beam and bridge girder with high slenderness ratio could be strengthened by adding a new channel cap on the top face or angle sections to the tips of the compression flange. By adding these members, the radius of gyration in the weak axis, r_y, increases with the same effective length factor of laterally unsupported length, l, that decreases the slenderness ratio l/r_y of the cross-section.

However, there is a lack of experimental and analytical research on the lateral torsional capacity of built-up cross-sections. The objective of this paper is to provide graphs to show the

[1] Design Engineer, Poe Engineering Inc., <sepehr.movaghati@gmail.com>

advantageous of welding angles to the compression flange of doubly symmetric beams to increase their LTB resistance and the beam serviceability.
To evaluate the investigated strengthened built-up sections, an FE model was developed using software ABAQUS (Hibbett, Karlsson, and Sorensen 1998) and validated by experimental test results of a universal I-shape beam section under uniform bending moment (Dibley 1969). A parametric study on the capacity of three different w-sections strengthened with two angles were studies and the results are presented.

Figure 1: Two monorail crane bridge girders supported on top-flange of runway beam

2. Literature Review

Various experimental and analytical investigations have been carried out to measure the LTB strength of structural members under flexure. The critical value of the moment is the major parameter to assess the stability of a beam under LTB. For an I-beam with two planes of symmetry which is bent in the plane of the greatest flexural rigidity, as long as the load on the beam is below the critical value $(M_0)_{cr}$, the beam will be stable (Timoshenko and Gere 1961). The critical moment causes instability can be calculated as:

$$(M_0)_{cr} = \frac{\pi}{l}\sqrt{EI_\eta C(1+\frac{C_1}{C}\frac{\pi^2}{l^2})} \quad (1)$$

Where C is the torsional rigidity, C_1 is the warping rigidity, E is the module of elasticity, l is the unbraced length of the beam, and I_η is the principal moment of inertia of the cross-section about the minor axis of bending. The inelastic LTB of steel members was also analytically calculated using differential equations (Galambos and Fukumoto 1963)(Timoshenko and Gere 1961).
The theoretical equations and design loads were verified and calibrated using experimental tests results. Early studies showed a good correlation between the theoretical and experimental bending strength values of slender simply supported beams which buckled in the elastic range (Hechtman et al. 1957). Many experimental studies were then performed to investigate the effect of different bracing conditions, as well as initial material and geometric imperfections in the inelastic beam buckling behavior (Dibley 1969), (Fukumoto, Kubo, and Itoh 1980), (Yoshida and Maegawa 1984) and (Wong-Chung and Kitipornchai 1987). The influence of major axis moment gradient on the capacity of beams was investigated experimentally (Dux and Kitipornchai 1983), (Wakabayashi and Nakamura 1983) and analytically (Helwig, Frank, and

Yura 1997). The moment gradient was later illustrated in the AISC specification (ANSI 2010)as the lateral-torsional buckling modification factor, C_b.

Influence of residual stresses on various instability, particularly inelastic buckling, where the presence of residual stresses affects the development of yield zones were studies as an initial nonlinearity (Nethercot 1974). In statistical studies, it was observed that the compressive residual stresses at the flange end reduce the ultimate strength (Fukumoto et al. 1980). Also, the presence of residual stresses in steel I-sections can have a significant effect upon the section's apparent St. Venant torsional rigidity (Nethercot 1974). Studies on the effect of different residual stress patterns in the LTB capacity of hot rolled and welded I-shape beams, (Nethercot 1974) concluded that the pattern of residual stresses presents within a section is not particularly significant in inelastic lateral buckling curve as the peak values of compressive and tensile residual flange stresses.

With the development of computational tools, the application of finite element models (FEMs) to calculate the flexural-torsional buckling strength and design formulation have been extended recently. Researchers studied the LTB capacity of rolled and welded shape beams (Kabir and Bhowmick 2018) (Subramanian and White 2017) and high-strength steel beam sections (Bradford and Liu 2016).

3. Design Approach

As specified in the AISC specification (ANSI 2010), the LTB resistance is related to the unbraced length of the beam, the section geometry, and the material properties. The nominal flexural strength, M_n, of the beams shall be the lower value obtained according to the limit states of yielding, lateral torsional buckling and local buckling. For a doubly symmetric compact I-shaped members M_n could be calculated based on three different unbraced length limits. For short span or closely braced beams, limit state of LTB does not apply. However, elastic or inelastic LTB may apply for more slender beams according to chapter F of AISC specification. The nominal flexural strength versus unbraced length based on the LRFD method for three different w-sections investigated in this study is plotted in Fig. 2. For torsion and flexure combination of more complex sections, chapter H of the specification and the commentary (ANSI 2010) require critical stress determination by elastic stress analysis based on established theories of structural mechanics (Seaburg and Carter 1997).

Serviceability limits are also considered for designing crane runway beams based on different crane classes. Fisher (Fisher 1984) suggested vertical deflection limit of span/600 without vertical impact for top running crane classes A, B and C, and span/400 for lateral deflections to avoid objectionable visual lateral movements.

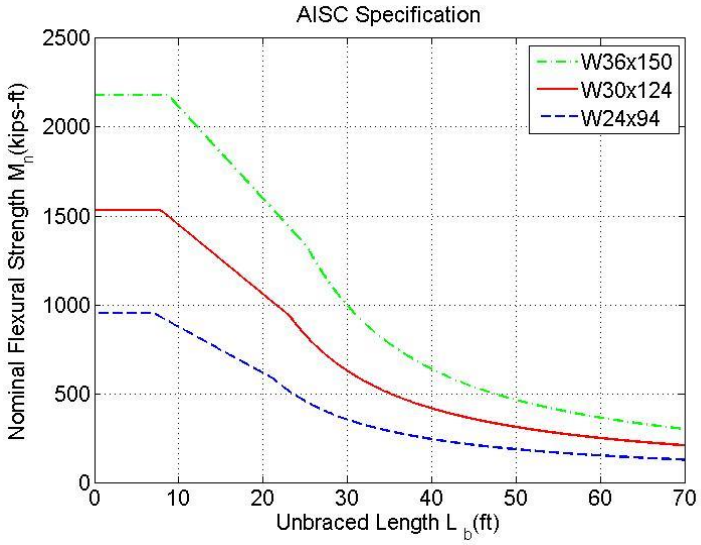

Figure 2: Nominal flexural strength about strong axis versus unbraced length (ANSI 2010)

3.1 Loading Configuration

According to the ASCE 7, standard for minimum design loads, the design load for runway beams shall include the maximum wheel loads of the crane and the vertical, lateral, and longitudinal impact forces induced by the moving crane. The maximum wheel loads of the crane to determine the induced vertical impact shall be increased by a percentage between 0% to 25% based on the type of crane. Moreover, the lateral load to the runway in combination with the vertical load shall be 20% of the sum of the rated capacity of the crane and the weight of the hoist and trolley. The lateral force shall be assumed to act horizontally at the traction surface of the beam. The load combination to design industrial building members are provided in the literature (AISE 1979)(Bakota 1977). As mentioned in the preceding section, the AISC specification approach to assign the biaxial flexural capacity of the beam section is presented in Chapter H (ANSI 2010).

4. Finite Element Modeling

A three-dimensional finite element model is developed using the finite element software ABAQUS (Hibbett et al. 1998). To simulate the instability of the beam section, continuum four node shell elements with reduced integration, 4-node S4R elements, with hourglass control are used. The beam flange width and beam height are meshed to 8 elements. Because of the impact lateral load on the beams, the effect of initial out of straightness in the response of the beam is negligible and not implemented.

4.1 Model Verification

To verify the developed FEM, the experimental test results on a series of universal I-section beams under a uniform bending moment were used (Dibley 1969). Two downward vertical loads at the beam ends with two vertical simple supports provide a uniform bending moment in the unbraced middle portion of the span. The supports provide restrain against lateral bending and rigid constraint against torsion. Material properties and initial imperfections similar to the experimental test were applied to the FE model. The bending moment capacity of universal beam section 12×4 UB 19, with the steel yield stress of 67ksi, and different unsupported lengths was calculated. The FE model can well predict the LTB capacity of the experimentally tested

specimens as summarized in Table 1 with the difference between the predicted capacity and the average experimental tests results.

Table 1: Verification of FEM

Section	L (in.) Unsupported span	a (in.) Moment arm	S_x (in.^{3}) Section Modulus	M_f[1] (kips-ft)	M_a[2] (kips-ft)	M_a/M_f
12×4 UB 19	148.4	75.8	22.5	69.8/63.8	64.4	0.96
12×4 UB 19	129.6	64.8	22.5	78.0/83.2	80.3	1.00
12×4 UB 19	82.4	41.2	22.5	125.1/119.1	123.5	1.01

1. maximum bending moment in test
2. maximum bending moment in FEM analysis

4.2 Material Properties

A bilinear elastoplastic stress-strain curve is used in all the models with nonlinear isotropic strain hardening of 1% of the elastic stiffness. The yield stresses for the parametric study are taken as 50 ksi and 36 ksi for w-section beam and angle section respectively. Also, the modulus of elasticity and Poisson's ratio are taken as 29000 ksi and 0.3, respectively. The self-weight of the steel material is not considered in the models.

4.3 Residual Stresses

During the fabrication of I-shape beam and angle sections, the steel is subjected to different cooling at different locations. The self-equilibrating internal stresses are affected by manufacturing condition, particularly cooling processes, known as residual stresses. Those parts of the section which cool rapidly, for example, the flange tips of an I-shape section, are usually left in residual compression, whilst residual tension is normally found in those regions which cool more slowly, such as the area of the web to flange junction (Nethercot 1974). The longitudinal residual stresses of rolled I-shape and angle sections were measured by sectioning method of flanges, web, and angle legs in experimental studies (Alpsten 1968) (ECCS 1985). In this study, Initial residual stresses are included in the models. compressive residual stresses at the flange tips and middle of the web are assumed in the order of 25% and 30% of the steel yield strength respectively (Fig. 3). Also, the longitudinal residual stresses in hot-rolled angles are assumed with a linear stress distribution with the peak value of 0.25 of the compressive yield stress at the angle toes and heel. At the fillet weld zone of the angle to the beam top flange connection, the steel is subjected to highly localized expansion and tension residual stresses and simulated in the FEMs per literature (Radaj 1992), (Masubuchi 2013), (Zinn and Scholtes 2002). In the FEMs, the residual stresses are applied by tension and compression stresses in the longitudinal direction as an initial condition and the stresses redistribute to attain an equilibrium.

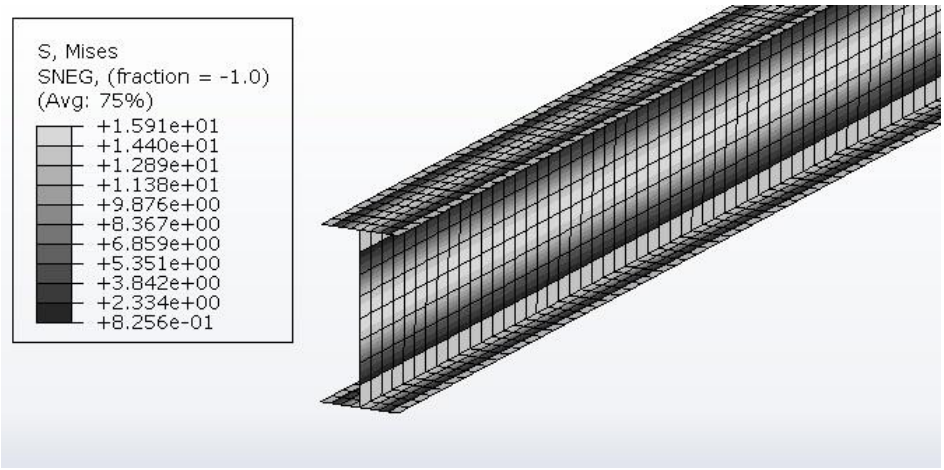

Figure 3: Initial longitudinal residual stresses in rolled I-shape section

4.4 Boundary Condition

The boundary conditions shown in Fig. 4 are incorporated into the finite element models by restraining the top and bottom nodes of the flanges at the beam ends against lateral and vertical deflections but allowing for the major and minor axis rotations and warping displacements. Tiebacks are used to connect the runway beam to the main structural frame to transfer the lateral load to the bracing system in industrial buildings.

4.5 Loading Configuration

The load per wheel is the total vertical and lateral loads divided by the total number of wheels. In this study, the longitudinal force from the impact load is not expected to generate the critical loading condition and is not applied in the model. Two concentrated point loads, 10-ft apart from each other, on the top flange of the I-shape sections is considered to represent the wheel loads shown in Fig. 4.

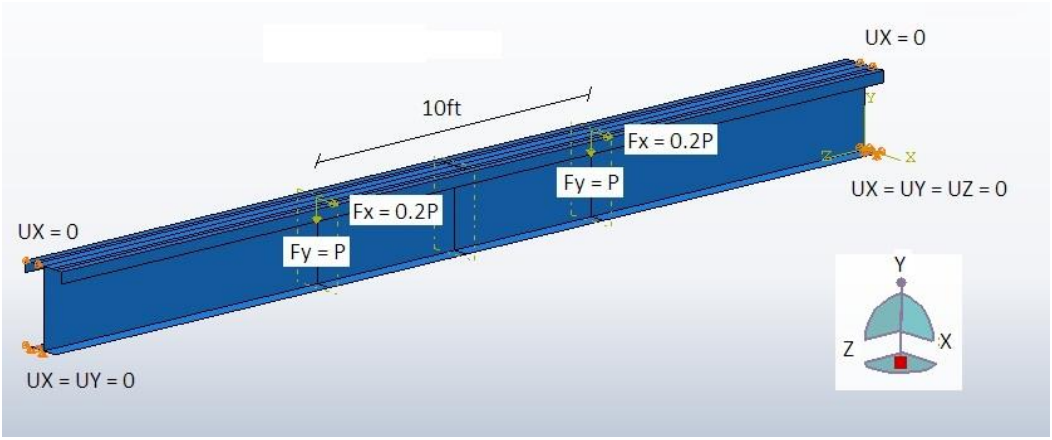

Figure 4: restrained nodes and concentrated point loads on FEM (model num. 14, see Table 4 for details)

5. Parametric Study

A total of 18 FE models with three different original I-shape sections and three different unbraced lengths (30-ft, 45-ft, and 60-ft) were developed and analyzed with the material properties, load configuration, and boundary conditions explained in section 4. The cross-

sectional details of the I-shape beams with the additional angles welded to the top flange of the beam section are shown in Fig. 5 and summarized in table 2 and table 3.

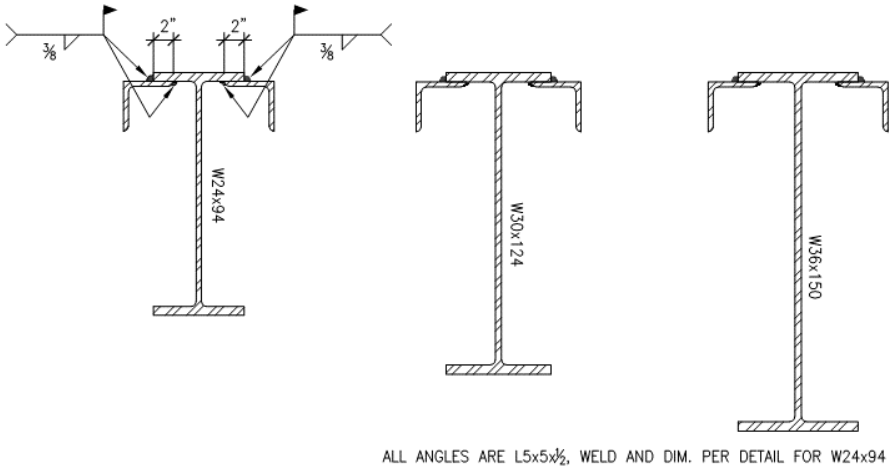

Figure 5: Cross-section of strengthened girders

Table 2: Cross-sectional properties of I-shape beams

Beam Section	d (in.) depth	t_w (in.) Web thickness	b_f (in.) Flange width	t_f (in.) Flange thickness	I_x (in.^{4}) Moment of inertia X-X	I_y (in.^{4}) Moment of inertia Y-Y
W24×94	24.3	0.515	9.07	0.875	2700	109
W30×124	30.2	0.585	10.5	0.930	5360	181
W36×150	35.9	0.625	12	0.940	9040	270

Table 3: Cross-sectional properties of angle

Section	I (in.^{3}) Moment of inertia	S (in.^{3}) Elastic section modulus	R (in.) Radius of gyration	J (in.^{4}) Torsional constant	C_W (in.^{6}) Warping constant
L5×5×1/2	11.3	3.15	1.53	0.417	0.744

5.1 Analysis Results

Nominal flexural strength of the studied I-shape sections versus the unbraced length per equations provided in AISC specification chapter F (ANSI 2010) is shown in Fig. 2. The analysis results of the developed sophisticated FEMs for the original I-shape beams and the built-up strengthened sections are provided in this section. Lateral torsional buckling occurred during the loading with the compressive top flange of the girder moved laterally at its midspan combined with the bending deformation caused by the lateral impact load (Fig. 6). The values of the vertical wheel load, P, for two different lateral deformation limit states are provided in table 4. P_{400} and P_{100} in this table represent the value of the concentrated loads applied on the beam section at the lateral deflection limit states of L/400 and L/100 respectively.

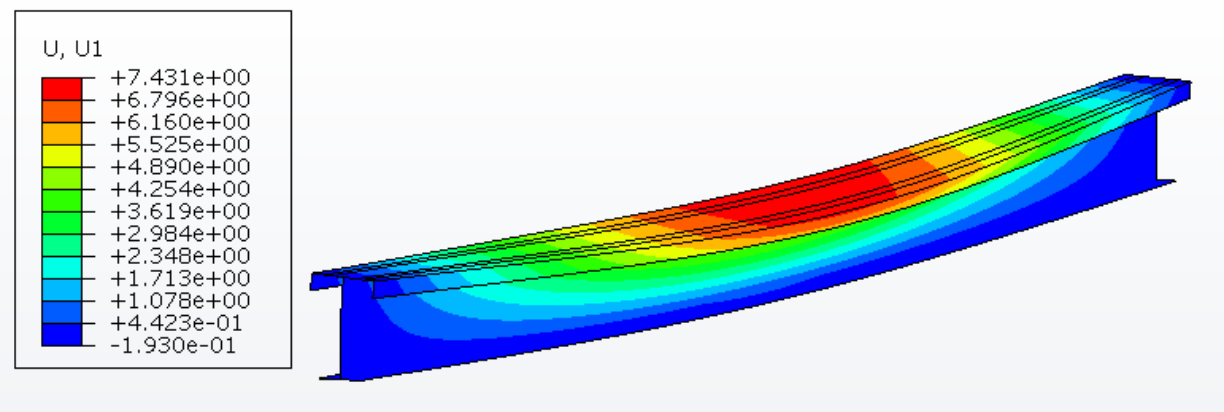

Figure 6: Deformed FEM (model num. 10, see Table 4 for details)

Table 4: Parametric study result

Model	I-shape	Angle	Unbraced length L (ft)	P_{400}[1] (kips)	P_{100}[2] (kips)	Load capacity ratio[3]
1	W24×94	-	30	5.8	15.5	-
2		L5×5×1/2	30	33.3	61.5	5.74,3.97
3		-	45	3.0	7.2	-
4		L5×5×1/2	45	14.2	27.3	4.73,3.79
5		-	60	1.9	4.4	-
6		L5×5×1/2	60	7.9	16.0	4.16,3.64
7	W30×124	-	30	8.7	23.4	-
8		L5×5×1/2	30	42.4	81.8	4.87,3.50
9		-	45	4.2	10.8	-
10		L5×5×1/2	45	18.0	36.1	4.29,3.34
11		-	60	2.7	6.5	-
12		L5×5×1/2	60	10.1	20.7	3.74,3.18
13	W36×150	-	30	11.9	32.8	-
14		L5×5×1/2	30	53.2	103.7	4.47,3.16
15		-	45	5.7	15.2	-
16		L5×5×1/2	45	22.4	46.4	3.93,3.05
17		-	60	3.6	8.8	-
18		L5×5×1/2	60	12.5	26.4	3.47,3.00

1. Crane wheel load per L/400 lateral deflection
2. Crane wheel load per L/100 lateral deflection
3. Load capacity ratio between original section and strengthened section for lateral deflection limit states of L/400 and L/100 respectively

The increases in loading capacity of strengthened sections are summarized in Table 4 and plotted versus the original I-shape sections load capacity in Fig. 7. According to the FE analysis results, welding L5×5×1/2 angles on both ends of the compression flange significantly increased the load bearing capacity of the original sections for the minimum of three times.

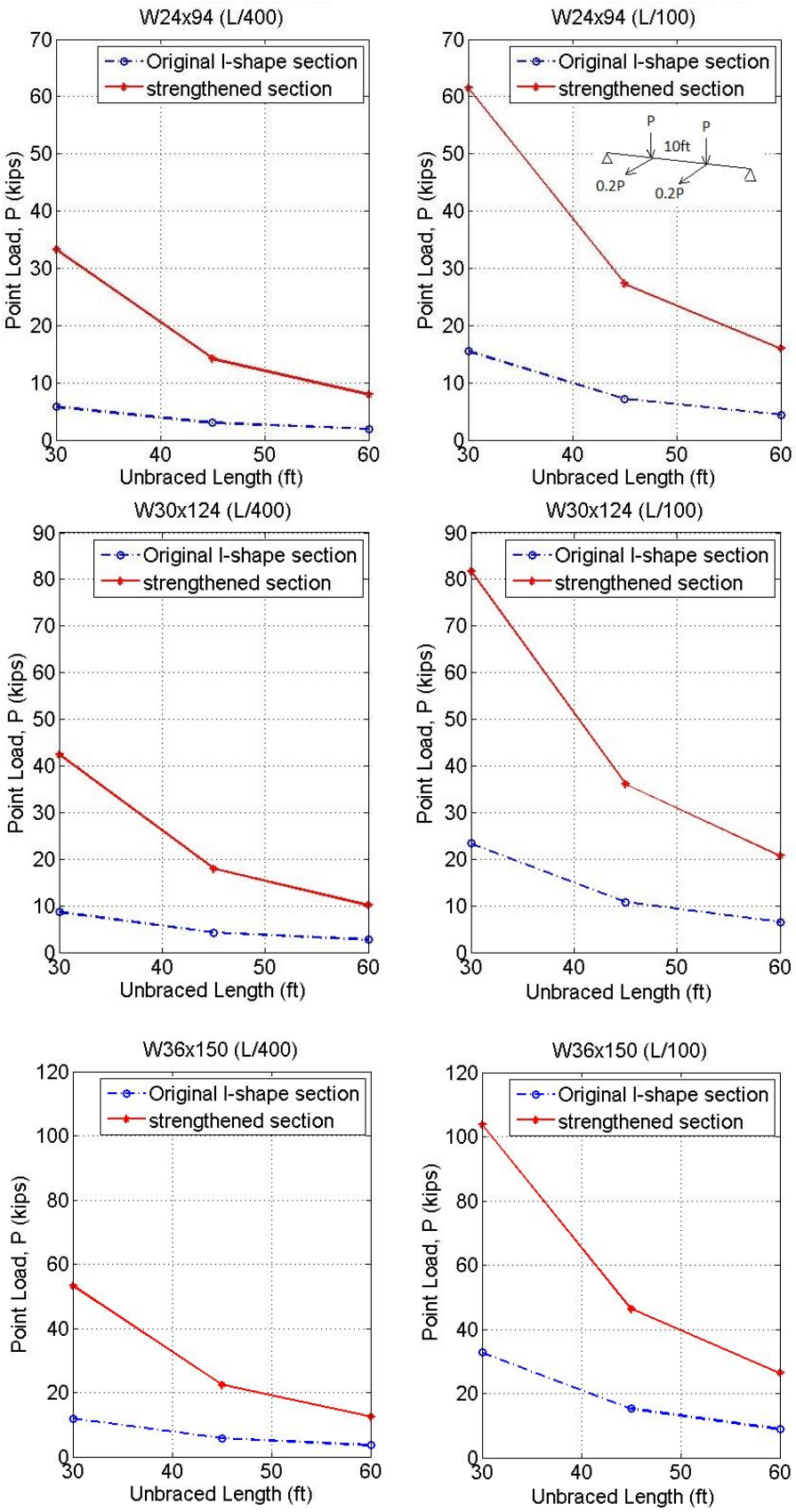

Figure 7: Crane wheel load P

6. Conclusion

In this paper the method strengthening industrial crane bridge girders and runway beams by welding angles to the tips of the compression flange were presented. Performing a parametric finite element analysis on three different I-shape sections proved that this method could be an efficient technic for strengthening class A or B cranes with a low number of lifts per day. The original beam sections with the nominal depth of 24-in, 30-ft and 36-in were modeled in software ABAQUS with shell elements considering the residual stresses. The load bearing capacity of the I-shape beams and the built-up strengthened sections with L5×5×1/2 angle welded to the compression flange tips were compared for three different unbraced length from 30-ft to 60-ft. The following items were concluded based on the crane wheel load on the girders at two lateral deflection limits of L/400 and L/100:

- The load capacity of the strengthened girders was increased significantly between 3.00 to 5.74 times the load capacity of the original I-shape sections.
- Higher increases in the load capacity were observed at the limit state corresponding to a lower lateral deflection.
- Strengthened beams with a shorter span gained more load capacity relative to the beams with the same cross-sectional properties but with a longer unbraced length.
- The load capacity ratio between the original and the strengthened beam section is higher for the beam sections with a smaller flexural moment of inertia.

It should be noted that for strengthening cranes with a higher number of lifts per day the potential occurrence of fatigue failure should also be investigated. Moreover, the runway beam connection to the main frame with tie backs and the main structural frame strength to support the runway beam should be analyzed and checked before increasing the rated capacity of a crane.

References

AISE. 1979. "*Guide for the Design and Construction of Mill Buildings AISE Technical Report No. 13*." Pittsburgh, Pa.: Association of Iron and Steel Engineers.

Alpsten, Goran A. 1968. "*Thermal Residual Stresses in Hot-Rolled Steel Members*." Lehigh university. Department of civil engineering.

ANSI, AISC. 2010. "AISC 360-10." *Chicago, IL*.

Bakota, Jhon F. 1977. "Mill Building Design Procedure." Engineering Journal-American Institute of Steel Construction Inc. 14(4):130–37.

Bradford, Mark A. and Xinpei Liu. 2016. "Flexural-Torsional Buckling of High-Strength Steel Beams." *Journal of Constructional Steel Research* 124:122–31.

Dibley, J. E. 1969. "lateral torsional buckling of I-sections in grade 55 steel." *Proceedings of the Institution of Civil Engineers* 43(4):599–627.

Dux, Peter F. and Sritawat Kitipornchai. 1983. "Inelastic Beam Buckling Experiments." *Journal of Constructional Steel Research* 3(1):3–9.

ECCS, CECM. 1985. "EKS." *Recommendation for Angles in Lattice Transmission Towers*.

Fisher, James M. 1984. "Industrial Buildings: Guidelines and Criteria." *Engineering Journal* 149–53.

Fukumoto, Yuhshi, Masahiro Kubo, and Yoshito Itoh. 1980. "Strength Variation of Laterally Unsupported Beams." *Journal of the Structural Division* 106(1):165–81.

Galambos, Theodore V and Yuhshi Fukumoto. 1963. *Inelastic Lateral-Torsional Buckling of Beam-Columns*. Fritz Engineering Laboratory, Lehigh University.

Hechtman, Robert A., John S. Hattrup, Eugene F. Styer, and John L. Tiedemann. 1957. "Lateral Buckling of Rolled Steel Beams." *Transactions of the American Society of Civil Engineers* 122(1):823–43.

Helwig, Todd A., Karl H. Frank, and Joseph A. Yura. 1997. "Lateral-Torsional Buckling of Singly Symmetric I-

Beams." *Journal of Structural Engineering* 123(9):1172–79.
Hibbett, Karlsson, and Sorensen. 1998. *ABAQUS/Standard: User's Manual*. Vol. 1. Hibbitt, Karlsson & Sorensen.
Kabir, Imran and Anjan K. Bhowmick. 2018. "Lateral Torsional Buckling of Welded Wide Flange Beams under Constant Moment." *Canadian Journal of Civil Engineering* 45(9):766–79.
Masubuchi, Koichi. 2013. *Analysis of Welded Structures: Residual Stresses, Distortion, and Their Consequences*. Vol. 33. Elsevier.
Nethercot, D. A. 1974. "Residual Stresses and Their Influence upon the Lateral Buckling of Rolled Steel Beams." *The Structural Engineer* 52(3):89–96.
Radaj, D. 1992. "Heat Effects of Welding Temperature Field, Residual Stress, Distortion."
Seaburg, Paul Allen and Charles J. Carter. 1997. *Torsional Analysis of Structural Steel Members*.
Subramanian, Lakshmi and Donald W. White. 2017. "Resolving the Disconnects between Lateral Torsional Buckling Experimental Tests, Test Simulations and Design Strength Equations." *Journal of Constructional Steel Research* 128:321–34.
Timoshenko, Stephen P. and James M. Gere. 1961. "Theory of Elastic Stability."
Wakabayashi, Minoru and Takeshi Nakamura. 1983. "Buckling of Laterally Braced Beams." *Engineering Structures* 5(2):108–18.
Wong-Chung, A. D. and S. Kitipornchai. 1987. "Partially Braced Inelastic Beam Buckling Experiments." *Journal of Constructional Steel Research* 7(3):189–211.
Yoshida, Hiroshi and Kouji Maegawa. 1984. "Lateral Instability of I-Beams with Imperfections." *Journal of Structural Engineering* 110(8):1875–92.
Zinn, W. and B. Scholtes. 2002. "Residual Stress Formation Processes during Welding and Joining,[in] Handbook of Residual Stress and Deformation of Steel, Edited by G." *Totten, M. Howes, and T. Inoue, ASM International, Ohio, USA* 391.